

Luneburg Lens Approach to Nuclear Rainbow Scattering

F. Michel,¹ G. Reidemeister,² and S. Ohkubo³

¹*Faculté des Sciences, Université de Mons-Hainaut, B-7000 Mons, Belgium*

²*Faculté des Sciences, Université Libre de Bruxelles, CP229, B-1050 Bruxelles, Belgium*

³*Department of Applied Science and Environment, Kochi Women's University, Kochi 780-8515, Japan*

(Received 5 March 2002; published 23 September 2002)

The physical interpretation of nuclear rainbow scattering within the frame of the optical model is critically investigated. Starting from the properties of the Luneburg lens, a gradient index device that displays refractive features similar to those of the nuclear potential, important differences between the mechanisms producing the nuclear and optical rainbows are pointed out.

DOI: 10.1103/PhysRevLett.89.152701

PACS numbers: 25.70.Bc, 03.65.Sq, 24.10.Ht

The optical model, in which the highly complicated nucleus-nucleus interaction is replaced by a complex two-body effective potential, plays a central role in the description of nucleus-nucleus scattering [1]. It has recently been found that, at incident energies of a few MeV per nucleon, several light heavy-ion systems, among which $^{16}\text{O} + ^{16}\text{O}$, $^{16}\text{O} + ^{12}\text{C}$, and $^{12}\text{C} + ^{12}\text{C}$ display more transparency than most neighboring systems, for which absorption at small and intermediate distances is nearly complete. Indeed, their elastic scattering angular distributions reveal unmistakable refractive features, such as rainbow scattering patterns and broad interference minima; the latter have come to be known in the literature as “Airy minima” [2]—a terminology to which, for convenience, we will stick in most of the following. These refractive features, which are contained in the farside contribution to the scattering amplitude [3], can be described consistently only by resorting to optical potentials with a deep (several hundreds MeV) real part.

In the theory of the meteorological rainbow [4], the primary bow owes its existence to the fact that the deflection angle of the rays reflected once inside a raindrop reaches an extremum for an impact parameter b equal to about $7/8$ of the radius of the drop. Airy structure, which appears on the lit side of the rainbow in the form of faint supernumerary bows, is associated with the interference between pairs of trajectories that lead to a same deflection angle, with an impact parameter, respectively, larger and smaller than that corresponding to the extremum of the deflection function.

The similarity of the pattern displayed by some light heavy-ion elastic scattering angular distributions, and the Airy structure observed in the meteorological rainbow, may look somewhat surprising in view of the important qualitative and quantitative differences between these two scattering systems. As a matter of fact, few studies have been devoted to a detailed investigation of the interrelation of the nuclear rainbow and Airy extrema with their optical counterparts. It is the purpose of this Letter to present a novel approach to the understanding of the nuclear rainbow and Airy structure; in particular, we

want to clarify the transition between the region of relatively high incident energies where rainbow scattering has set in and lower energies where rainbow scattering is not yet observed but the nuclear “Airy minima” are clearly present.

Most of the forthcoming discussion will center on calculations performed by discarding the imaginary part of the potential; indeed, the rainbow pattern and Airy structure are largely insensitive to a reduction of the absorption: in most cases, the rainbow angle and the angular position of the Airy minima do hardly change, even when the potential is made purely real ([5]; see also Fig. 1). The second simplification will be to discuss the

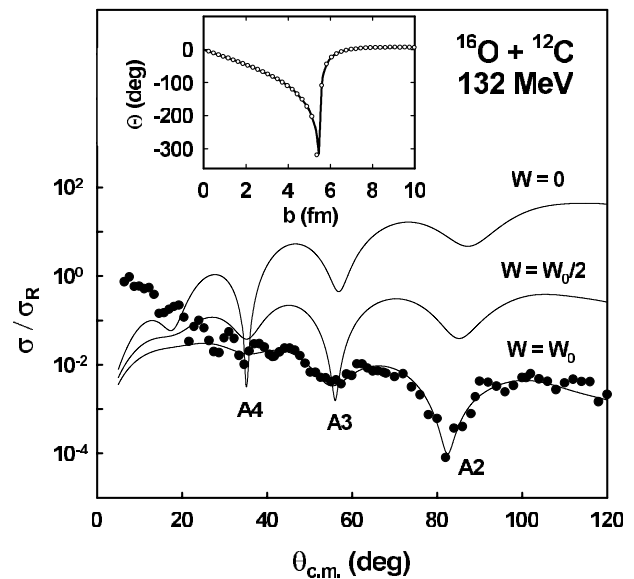


FIG. 1. Effect on the position of the “Airy minima” of the farside contribution to elastic scattering (labeled A_2 , A_3 , and A_4 ; full lines) of a reduction of the nominal absorption of the optical model potential used by Ogloblin *et al.* [5] to describe their $^{16}\text{O} + ^{12}\text{C}$ data at 132 MeV (dots). Inset: comparison of the classical (full line) and quantum mechanical (open circles) deflection function calculated with the real part of the same potential (adapted from [6]).

physics of the nuclear Airy structure in terms of the interference between *classical* trajectories leading to the same scattering angle; this is justified by the fact that for a purely real interaction potential, the quantum deflection function calculated from the (real) phase shifts for the systems investigated here is very close to its classical limit [6] (Fig. 1). The remarkable success of semiclassical approaches also points to the pertinence of the concept of trajectory in the description of light-ion and light heavy-ion scattering down to relatively low energies. Thus in the so-called barrier-wave/internal-wave approach of Brink and Takigawa [7] (which supposes that the real part of the effective potential displays a “pocket” at small distances for all the active partial waves, a condition which is fulfilled up to relatively high incident energy for the deep potentials considered here), the elastic scattering amplitude is split into two contributions, corresponding, respectively, to the part of the flux which is reflected at the potential barrier, and that which crosses the barrier and is reflected at the most internal turning point of the effective potential. The Airy oscillations seen in the elastic $^{16}\text{O} + ^{16}\text{O}$ angular distributions for energies of 5 to 10 MeV per nucleon are due to the interference between these two contributions [8], each of which behaves smoothly in the angular region where the Airy oscillations are observed.

The classical trajectory of a material particle of energy E moving in a potential V and that of a light ray propagating in a medium with refractive index n are identical provided [9]

$$n = \sqrt{1 - \frac{V}{E}} \quad (1)$$

The potential corresponding to the propagation of light in a raindrop is a square well. Nussenzveig [10,11] has studied high frequency scattering of a scalar plane wave from a transparent sphere in great detail; using the Watson transformation he was able to expand the scattering amplitude into a multiple scattering (Debye) series, where each successive term is associated with an increasing number of refracted rays inside the sphere. Thus the first two terms ($p = 0, 1$) correspond, respectively, to direct reflection at the surface of the sphere and to direct transmission without any internal reflection; the usual rainbow and the secondary rainbow are associated, respectively, with the third and fourth terms of this series ($p = 2, 3$). In the potential picture, all the terms of the series, except the second one, involve nonclassical reflections; for example, the $p = 0$ term corresponds in the mechanical picture to a reflection at the potential discontinuity, at an incident energy higher than the effective potential barrier: this typical wave effect is especially enhanced at sharp boundaries like that of a square well.

The square well potential associated with the raindrop, and optical potentials used in the description of light

heavy-ion scattering, display several important differences: (i) The refractive index corresponding to the central part of the optical potential is much higher than that ($n = 1.33$) of water: the depth at the origin of the real part of the $^{16}\text{O} + ^{16}\text{O}$ potential of Khoa *et al.* [12], at 145 MeV incident energy, is about 350 MeV, which corresponds to a central refractive index ($n \approx 2.4$) comparable to that of diamond; (ii) the real part of the optical potential at small and intermediate distances is not constant; for example, the highly successful folding model potential [13] is much better approximated by a harmonic oscillator potential: the nuclear medium resembles less a crystal ball with a constant refractive index than a gradient index (GRIN) lens [14]; (iii) the surface of the real part of the optical potential is diffuse, which should reduce the importance of nonclassical reflections; (iv) the nuclear interaction includes a Coulomb repulsive term; for light-ion and light heavy-ion scattering, Coulomb effects are qualitatively not very important, except at small angles; these will be discarded in the rest of the discussion; (v) absorption, which is negligible in the meteorological case, is an important feature in nuclear scattering; as stated above this difference does, however, not seem to be decisive in the discussion of rainbow and Airy phenomena.

A particular GRIN lens, the so-called Luneburg lens [14], has a refractive index profile that approximates nicely that of the real part of the nuclear optical potential at small and intermediate distances. This spherical lens—whose refractive index n at the surface equals that of the surrounding medium, which we will suppose to be vacuum—produces perfect focusing, *inside* or *outside* the lens, of a beam of incident parallel light rays. In the case of internal focusing, the refractive index profile is [14]

$$n^2(r \leq R) = \frac{r_1^2 - r^2 + R^2}{r_1^2}, \quad n(r > R) = 1, \quad (2)$$

where R is the radius of the lens, and $r_1 < R$ is the distance of the focus to the center of the lens. Using Eq. (1) one obtains for the potential having equivalent properties

$$\begin{aligned} V(r \leq R) &= V_0 \left(\frac{r^2}{R^2} - 1 \right), & V_0 &= E \left(\frac{R}{r_1} \right)^2, \\ V(r > R) &= 0, \end{aligned} \quad (3)$$

that is, a truncated harmonic oscillator potential, which we will call in the present context a “Luneburg potential.” The focus moves away from the origin when energy increases:

$$r_1(E) = \frac{R}{\sqrt{V_0}} \sqrt{E}; \quad (4)$$

at the critical energy $E_{\text{crit}} = V_0$ the focus reaches the surface of the sphere ($r_1 = R$).

The focusing properties of the optical model potential have recently been studied for light-ion systems displaying incomplete absorption [15], for which a conspicuous focus appears in the probability density associated with the scattering wave function. A comparison of the $^{16}\text{O} + ^{16}\text{O}$ folding model potential used by Nicoli *et al.* [16] at 75 MeV, with an “osculating” Luneburg potential (with parameters $V_0 = 310$ MeV, $R = 4.8$ fm), is presented in Fig. 2, together with the classical trajectories associated with these two potentials. The focusing properties of the two potentials are seen to be closely similar. Of course, the external trajectories of the latter, which has a different surface behavior, are qualitatively different; we will come back to that point later.

The classical deflection angle associated with a Luneburg potential for $E < E_{\text{crit}}$ is a monotonic function of the impact parameter; the maximum deflection angle, which corresponds to a grazing trajectory ($b = R$), is equal to π . The deflection function has thus only one branch (Fig. 3), which is associated with an *internal* contribution to the scattering: the turning points corresponding to the barrier contribution ($b > R$) are located outside the range R of the potential, and the associated

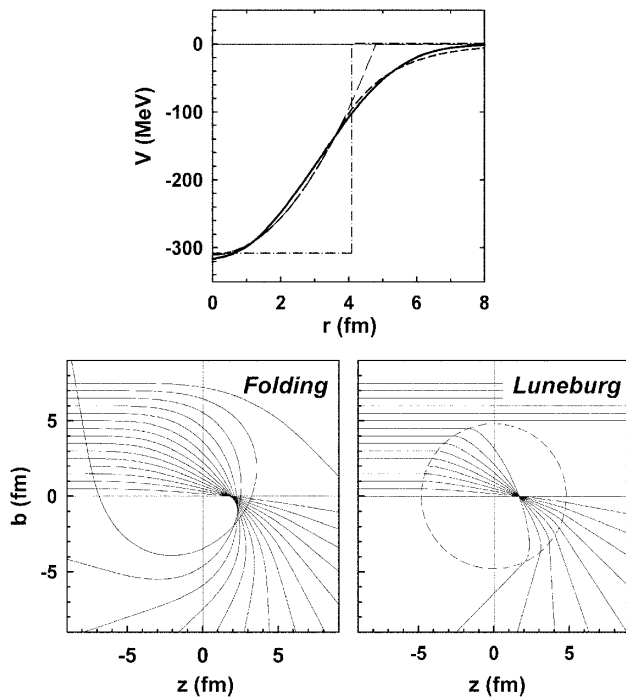


FIG. 2. Top: comparison of the $^{16}\text{O} + ^{16}\text{O}$ folding potential of Nicoli *et al.* [16] (full line) with a square well, and with a Luneburg potential ($V_0 = 310$ MeV, $R = 4.8$ fm, long dashed line) and its smooth-edge version ($\rho = 3.6$ fm, short dashed line). Bottom: classical trajectories for the $^{16}\text{O} + ^{16}\text{O}$ system at 75 MeV incident energy, calculated using the folding potential of Nicoli *et al.* [16] (left) and the Luneburg potential with radius $R = 4.8$ fm (cf. dashed line, right) (the Coulomb interaction has been switched off).

trajectories are not deflected. Since the deflection function has no extremum and has only one branch, no rainbow nor interference structure can be produced.

Although the shape of the Luneburg potential approximates that of realistic nuclear potentials much better than a square well, it has obviously an inadequate behavior in the surface region. The surface behavior of the nuclear potential can be simulated by introducing a cutoff $\rho < R$, beyond which an exponential tail is smoothly connected; the choice $\rho = 3.6$ fm brings this “smooth-edge Luneburg potential” in very good agreement with the 75 MeV $^{16}\text{O} + ^{16}\text{O}$ nuclear potential on the whole radial range (Fig. 2), and the classical trajectories calculated with this potential become nearly indistinguishable from those obtained with the real part of the nuclear potential. Because the potential has now become an “imperfect Luneburg potential,” some astigmatism is observed; in particular, trajectories passing in the outskirts of the potential, especially those with a distance of closest approach larger than R , are deflected at angles smaller than some trajectories with a smaller impact parameter; as a result the deflection function acquires a second branch for large impact parameters (Fig. 3). At low energy, the effective potential curves associated with this smooth-edge potential display a pocket, separated from the outside region by a smooth barrier maximum, and at the “grazing impact parameter” b_{gr} , for which the top of the barrier is exactly equal to the incident energy, orbiting, as discussed, e.g., by Ford and Wheeler [17], occurs. At low energy, the two branches of the classical deflection function are thus now separated by a singularity at b_{gr} (Fig. 3; each branch diverges logarithmically there [17]); this is a well-documented situation, e.g., in molecular collision physics [18]. As the deflection function has no genuine extremum, it still does not produce rainbow scattering; however, the presence of the second

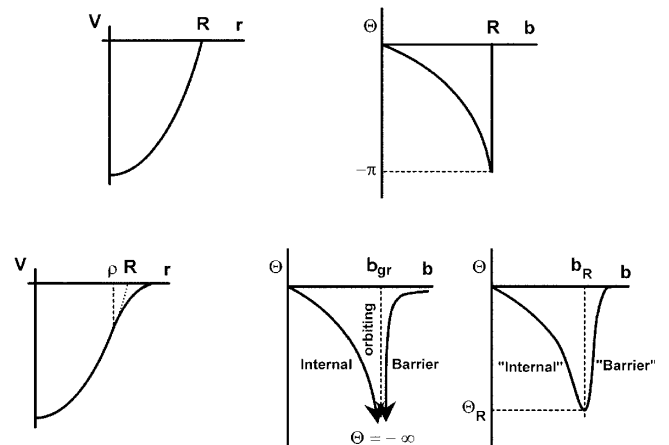


FIG. 3. Schematic representation of a Luneburg potential and its classical deflection function for $E < E_{\text{crit}}$ (top); a smooth-edge Luneburg potential and its semiclassical deflection function for $E < E_{\rho}^{\text{crit}}$ and $E > E_{\rho}^{\text{crit}}$ (bottom).

branch now makes possible the appearance of interference effects, and thus of Airy-like structure. The above discussion shows that classical trajectories with an impact parameter higher (lower) than b_{gr} are nothing else than barrier (internal) trajectories, respectively, in agreement with the interpretation of Ref. [8].

There exists a critical energy E_{ρ}^{crit} where the effective potential associated with the imperfect Luneburg potential loses its pocket at the grazing impact parameter [because the introduction of the exponential tail has lowered the barriers of the (bare) Luneburg effective potentials, this energy is lower than E_{crit}]. Above that energy, which in the $^{16}\text{O} + ^{16}\text{O}$ case is about 60 MeV (c.m.), orbiting disappears, and the deflection function becomes a continuous function of the impact parameter; with its two branches separated by an extremum (at $\Theta = \Theta_R$, Fig. 3), this deflection function can now generate rainbow scattering *and* genuine Airy oscillations. Although each of these (continuously connected) branches can no more strictly be associated with a barrier or an internal contribution, it is clear that there is perfect continuity between the two energy regimes.

The nuclear rainbow is not a perfect analog of the ($p = 2$) meteorological rainbow, for which one (“nonclassical”) reflection takes place within the drop: it corresponds to the second ($p = 1$) term in Nussenzveig’s expansion [10], where the only active mechanism is refraction. Another way to convince oneself of the dissimilarity of the nuclear and meteorological rainbows is to observe that their lit sides stand on opposite sides of the rainbow. The rainbow observed in nuclear physics is thus closely related to the so-called “zero-order rainbow” [19] of Newton, who believed in its existence (at an angular distance of the sun of only 26°), and thought it was difficult to observe because of the sun glare; however, because the $p = 1$ deflection function for the square well is monotonic, this rainbow is, in fact, inexistent as a meteor [19], but it eventually comes to life in nuclear scattering.

To conclude this discussion, we comment on the use of the Airy terminology to describe the interference structure seen in elastic light-ion and light heavy-ion scattering. This interference, like in the meteorological case, involves the two branches of the classical deflection function; however, at low energy, the origin of the second (barrier) branch is very different in the nuclear case, since it owes its existence to the diffuse tail of the potential, a phenomenon obviously not present in the meteorological rainbow, where the two branches of the $p = 2$ contribution are associated with qualitatively similar trajectories. Moreover, the interference minima seen at low energy are independent from the existence of a nuclear rainbow. From that point of view, calling these minima “Airy

minima” is misleading; “pre-rainbow interference minima” could be a more suitable terminology.

As energy increases, the deflection function acquires a genuine extremum, and a parabolic approximation to the deflection function around this minimum becomes progressively more justified; as a result the general structure of the differential cross section in the region of the rainbow angle is now adequately represented by the square of an Airy function [17]. However, the “Airy minima” observed in this case are those accompanying a $p = 1$ “nuclear Newton’s zero-order rainbow,” a phenomenon whose existence still relies on the diffuse tail of the nuclear potential; this feature of the nuclear potential makes at the same time a nuclear analog of the $p = 2$ meteorological rainbow unobservable, since the additional internal reflection needed for producing it would require a much sharper nuclear surface.

-
- [1] See, e.g., G. R. Satchler, *Direct Nuclear Reactions* (Clarendon Press, Oxford, 1983).
 - [2] See, e.g., S. Szilner *et al.*, Phys. Rev. C **64**, 064614 (2001), and references therein.
 - [3] R. C. Fuller, Phys. Rev. C **12**, 1561 (1975).
 - [4] H. M. Nussenzveig, Sci. Am. **236**, 116 (1977).
 - [5] A. A. Ogloblin *et al.*, Phys. Rev. C **62**, 044601 (2000); M. E. Brandan *et al.*, Nucl. Phys. **A688**, 659 (2001).
 - [6] R. Anni, Eur. Phys. J. A (to be published).
 - [7] D. M. Brink, *Semi-Classical Methods in Nucleus-Nucleus Scattering* (Cambridge University Press, Cambridge, 1985).
 - [8] F. Michel, F. Brau, G. Reidemeister, and S. Ohkubo, Phys. Rev. Lett. **85**, 1823 (2000); F. Michel, G. Reidemeister, and S. Ohkubo, Phys. Rev. C **63**, 034620 (2001).
 - [9] M. Born and E. Wolf, *Principles of Optics* (Cambridge University Press, Cambridge, 1999).
 - [10] H. M. Nussenzveig, J. Math. Phys. (N.Y.) **10**, 82 (1969); **10**, 125 (1969).
 - [11] H. M. Nussenzveig, *Diffraction Effects in Semiclassical Scattering* (Cambridge University Press, Cambridge, 1992).
 - [12] D. T. Khoa, W. von Oertzen, H. G. Bohlen, and F. Nuoffer, Nucl. Phys. **A672**, 387 (2000).
 - [13] See, e.g., M. E. Brandan and G. R. Satchler, Phys. Rep. **285**, 143 (1997).
 - [14] J. M. Gordon, Appl. Opt. **39**, 3825 (2000).
 - [15] F. Brau, F. Michel, and G. Reidemeister, Phys. Rev. C **57**, 1386 (1998).
 - [16] M. P. Nicoli *et al.*, Phys. Rev. C **60**, 064608 (1999).
 - [17] See, e.g., K. W. Ford and J. A. Wheeler, Ann. Phys. (N.Y.) **7**, 259 (1959).
 - [18] See, e.g., M. S. Child, *Molecular Collision Theory* (Academic Press, New York, 1984).
 - [19] C. F. Bohren and A. B. Fraser, Am. J. Phys. **59**, 325 (1991).